Received: 3 July 2019 | Revised: 11 September 2019 | Accepted: 16 September 2019

DOI: 10.1111/ter.12428

PAPER

Terra Nova WILEY

Salt décollement and rift inheritance controls on crustal deformation in orogens

Arjan R. Grool[1,2] | Ritske S. Huismans[1] | Mary Ford[2]

[1]Department of Earth Science, University of Bergen, Bergen, Norway

[2]CRPG, UMR 7358, Vandœvre-lès-Nancy, France

Correspondence
Arjan R. Grool, CRPG, 15 Rue Notre Dame des Pauvres, 54501 Vandœvre-lès-Nancy, France
Email: arjan.grool@univ-lorraine.fr

Funding information
Agence Nationale de la Recherche, Grant/Award Number: ANR-11-BS56-0031; Uninett SIGMA2, Grant/Award Number: NN44704K

Abstract

We investigate the factors that control the shortening distribution and its evolution through time in orogenic belts using numerical models. We present self-consistent high-resolution numerical models that simulate the inversion of a rift to generate an upper crustal antiformal stack, a wide outer pro-wedge fold-and-thrust belt, characterised by a two-phase evolution with early symmetric inversion followed by formation of an asymmetric doubly-vergent orogen. We show that a weak viscous salt décollement promotes gravitational collapse of the cover. When combined with efficient erosion of the orogenic core and sedimentation in adjacent forelands, it ensures the thick-skinned pro-wedge taper remains subcritical, promoting formation of an upper crustal antiformal stack. Rift inheritance promotes a two-phase shortening distribution evolution regardless of the shallow structure and other factors. Comparison to the Pyrenees strongly suggests that this combination of factors led to a very similar evolution and structural style.

1 | INTRODUCTION

A crustal-scale antiformal stack is a duplex of crustal thrust sheets with high overlap such that the roof thrust becomes folded into an anticlinal shape (e.g., Mitra & Boyer, 1986). Such a structure is observed in the Pyrenean Axial Zone (e.g., Muñoz, 1992) and the Alpine Lepontine dome (e.g., Schmid, Kissling, Diehl, Hinsbergen, & Molli, 2017). Formation of such significant structures remains poorly understood, but requires high internal shortening in response to a subcritical wedge taper. This can be achieved by either increasing critical taper or lowering the surface slope. Proposed mechanisms include a lateral strength increase of the mid-crustal décollement (Beaumont, Muñoz, Hamilton, & Fullsack, 2000), erosion of the internal orogen (Rushlow, Barnes, Ehlers, & Vergés, 2013) or sediment blanketing of the tip of the thick-skinned wedge (Sinclair, Gibson, Naylor, & Morris, 2005). During orogenesis the distribution of shortening between pro- and retro-wedges may change significantly and can describe two clear phases: early symmetric inversion followed by asymmetric doubly-vergent collision. Extensional inheritance likely plays a key role, as shown qualitatively by (Erdős, Huismans, van der Beek, & Thieulot 2014).

Analogue and numerical models show that primary controlling factors of the lithospheric scale structural style of deformation in an orogen are rheology of the crust and mantle (e.g., Burg & Gerya, 2005), strain weakening (e.g., Warren, Beaumont, & Jamieson, 2008), convergence rate (e.g., Faccenda, Gerya, & Chakraborty, 2008) and inherited weakness zones (e.g., Beaumont et al., 2000). Noteworthy secondary factors are erosion and sedimentation (e.g., Storti & McClay, 1995; Willett, 1999), which remove mass from the internal orogen and add mass to the distal wedges, reducing the surface slope and thereby altering where shortening will be accommodated.

Décollement rheology is known to influence critical taper and the distribution of shortening in the overlying wedge (e.g., Davis & Engelder, 1985; Ford, 2004). However, can a salt décollement also influence crustal deformation in the orogen as a whole? Efficient decoupling of the sedimentary cover might allow thin-skinned deformation to sufficiently change mass distribution at shallow depths to affect the crustal deformation in a manner similar to surface processes (Nilfouroushan, Pysklywec, Cruden, & Koyi, 2013). Could a

highly mobile cover trigger formation of an antiformal stack, and/or change distribution of crustal shortening?

Here, we build on previous work (Erdős et al., 2014; Erdős, Huismans, & van der Beek, 2015) that investigates the role of rift inheritance and surface processes using lithosphere scale high-resolution 2D thermo-mechanical models. Critically, we use a highly mobile cover (viscous salt décollement layer) instead of the moderately mobile cover (frictional-plastic décollement layer) used by Erdős et al. (2014), Erdős et al. (2015). To investigate the combined effect of rift inheritance and a highly mobile cover we present a novel measurement of the shortening distribution between the pro- and retro-wedges through time (Data S1). We compare our results with the Pyrenees, an orogen with a crustal-scale antiformal stack (e.g., Muñoz, 1992) and two-phase shortening distribution, and where a similar shortening distribution analysis was performed (Grool et al., 2018).

2 | METHODS

We use a modified 2D version of FANTOM (see Data S1), a high resolution (500 × 200 m in upper 25 km), thermo-mechanically coupled, arbitrary Lagrangian-Eulerian finite element code (Thieulot, 2011; Erdős et al., 2014). Localisation of deformation is incorporated through strain weakening of frictional-plastic materials. Surface processes were included with simple algorithms for elevation-dependent erosion and sedimentation up to 0 m base level.

Our models consist of a laterally homogeneous continental crust, comprising 3 km of pre-orogenic sediments underlain by a 1 km thick décollement layer, 21 km of upper crust and 10 km of strong lower crust (Figure 1). The lithospheric mantle extends to 120 km depth and sub-lithospheric mantle to 600 km depth. Convergence is imposed on both sides for a total convergence rate of 10 km/My. Initial localisation of deformation is seeded by a small weak seed at the top of the lower crust. Rift inheritance is generated by first extending for 50 km (e.g., Jammes & Huismans, 2012). Model 1 has a highly mobile cover with a weak viscous décollement layer representing salt with an effective viscosity of $\eta_{eff} = 10^{19}$ Pa·s. To show the influence of décollement rheology and rift inheritance, supplementary models S1 and S2 use a weak frictional décollement ($\phi_{eff} = 2°$) that is at least 10 times stronger than the décollement in Model 1 and no rift inheritance, respectively. The supplementary models are similar to earlier work (Erdős et al., 2014; Erdős et al., 2015) and are included for comparison with Model 1 and for new quantitative analysis of the shortening distribution between pro- and retro-wedges.

3 | RESULTS

3.1 | Effects of salt, surface processes and extensional inheritance

Model 1 is characterised by a three-phase evolution. Phase 0 is the pre-orogenic rift phase, where at t = 5 My, 50 km of extension results in a narrow, roughly symmetrical rift bounded by two sets of conjugate frictional-plastic shear zones that are seeded in the lower crust, one through the upper crust and one through the lithospheric mantle (Figure 2a). The pre-rift sedimentary cover has slid off the rift margins. No sediments were deposited in the rift.

Phase 1 initial lithospheric shortening leads to symmetric inversion of the rift zone. Inherited extensional shear zones are preferentially reactivated during the first 25 km of convergence, restoring crustal thickness, followed by uplift of a symmetric central block

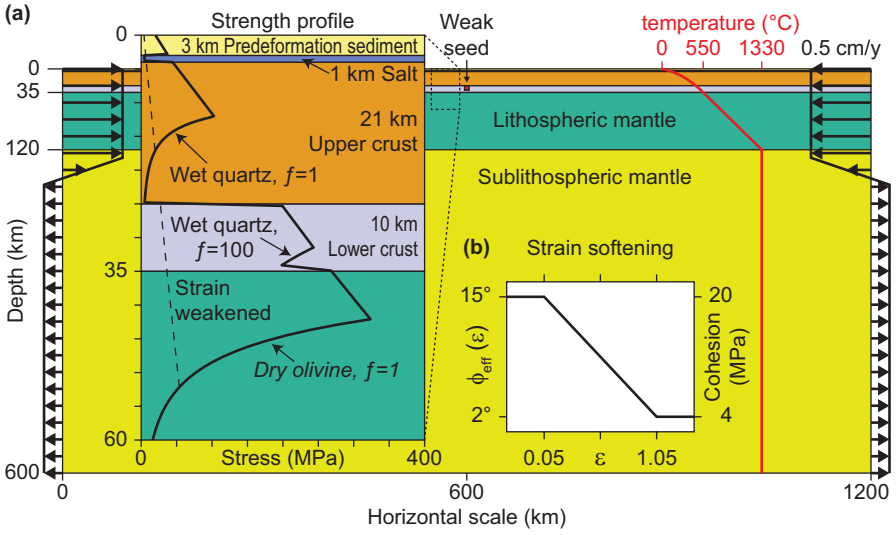

FIGURE 1 (a) Model geometry showing layer thickness, initial strength profile indicating the strong coupling of the lower crust and lithospheric mantle, thermal profile and velocity boundary conditions. The model's resolution is 500 × 200 m in the top 25 km, 500 × 800 m in the 100 km below that and 500 × 9800 m for the remaining 475 km. (b) Strain weakening of frictional materials is simulated by linearly reducing effective angle of internal friction ϕ_{eff} from 15° to 2° and cohesion C from 20 MPa to 4 MPa with increasing strain ε in the range $0.05 < \varepsilon < 1.05$

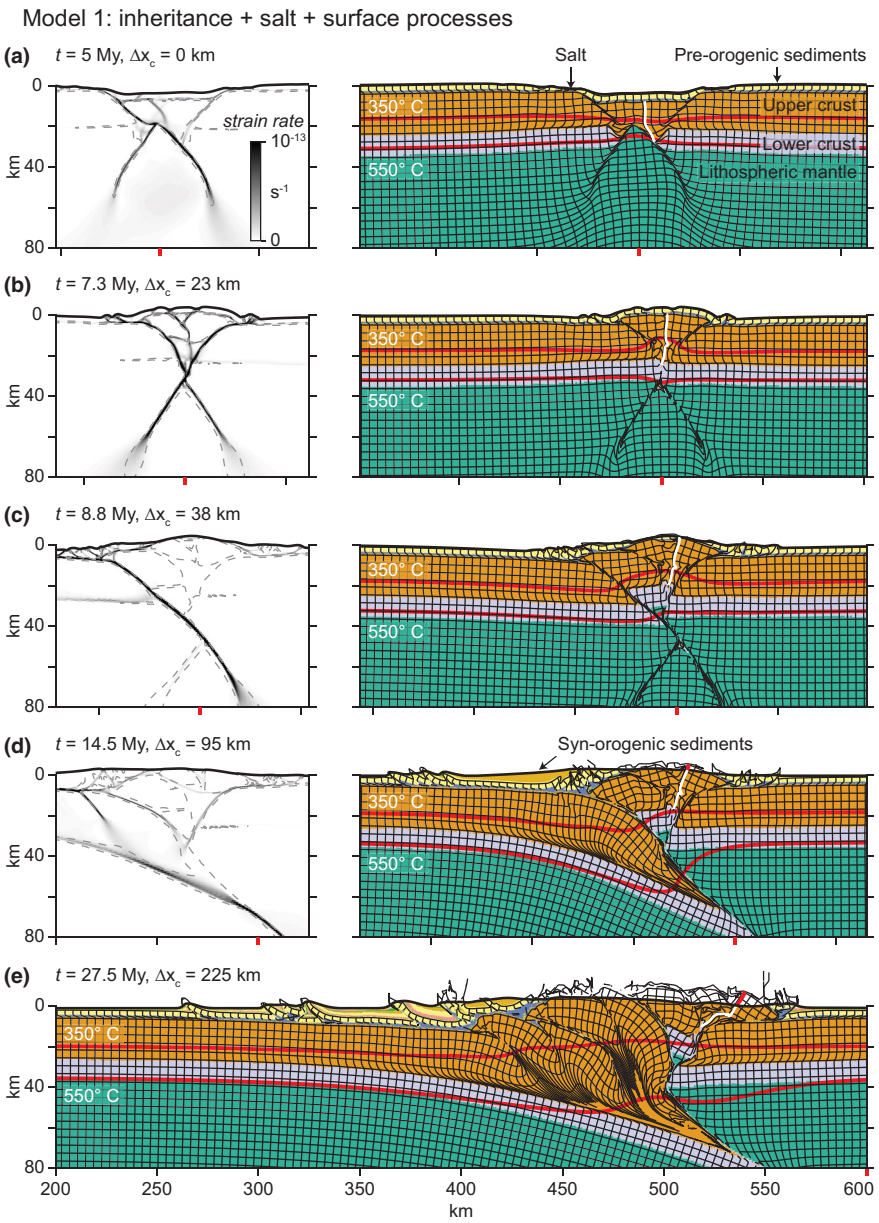

FIGURE 2 Evolution of Model 1, with a weak viscous salt décollement and extensional inheritance. The white line at the centre is tracked to measure the shortening distribution, ignoring the red part above topography. Strain rate plots (left) show the square root of the second invariant of the deviatoric strain rate tensor. Grey dashed lines mark fully strain weakened areas. (a) Rift phase. (b) Symmetric inversion. (c) Onset of collision and asymmetry, retro-wedge abandoned. (d) Retro-wedge reactivated and dominant wide thin-skinned outer pro-wedge fold-and-thrust belt. (e) Final configuration. Well-developed retro-wedge, antiformal pro-wedge and wide thin-skinned outer pro-wedge fold-and-thrust belt

(Figure 2b). The strain rate plot shows that both conjugate shear zones in the upper crust and upper mantle lithosphere are active simultaneously during this phase.

An asymmetric orogen develops during Phase 2 (Figure 2c, d, e). Strain localisation on a single large-scale shear zone initiates asymmetric subduction of lower crust and mantle lithosphere and abandonment of other, previously active shear zones (Figure 2c). Initial narrow thin-skinned fold-and-thrust belts not only root back into the deep shear zones, but also link to the gravitationally unstable cover that slides off the uplifting keystone block. At t = 14.5 My and 95 km of convergence, syn-orogenic sedimentation in a wedge-top basin promotes wide thin-skinned thrust sheets in the outer pro-wedge (Figure 2d). Below and at the same time, thick-skinned deformation propagates outward along the mid-crustal décollement due to progressive growth of the pro-wedge. As the crustal antiformal stack grows, over-steepening of its trailing edge reactivates the retro-wedge (Figure 2d).

After 225 km of convergence (27.5 My; Figure 2e) the thin-skinned pro-wedge fold-and-thrust belt has efficiently propagated outward. The crustal antiformal stack continues to grow by frontal accretion of thrust sheets while the uplifting internal zone is continually eroded.

The contrasting behaviour of models with a less efficient décollement horizon and no extensional inheritance is illustrated in Data models S1 and S2 (Figure 3). Model S1 is identical to Model 1 except a stronger frictional décollement. It exhibits a clear coupling between shallow and deep structures. Thin-skinned leading edge structures root back into an active crustal-scale shear zone, before being carried passively above the next crustal imbricate as deformation propagates forward. The décollement level is therefore active only at its leading edge, linking back to a single crustal structure. In contrast with Model 1, an antiformal stack does not form (Figure 3a). However, retro-wedge development is very

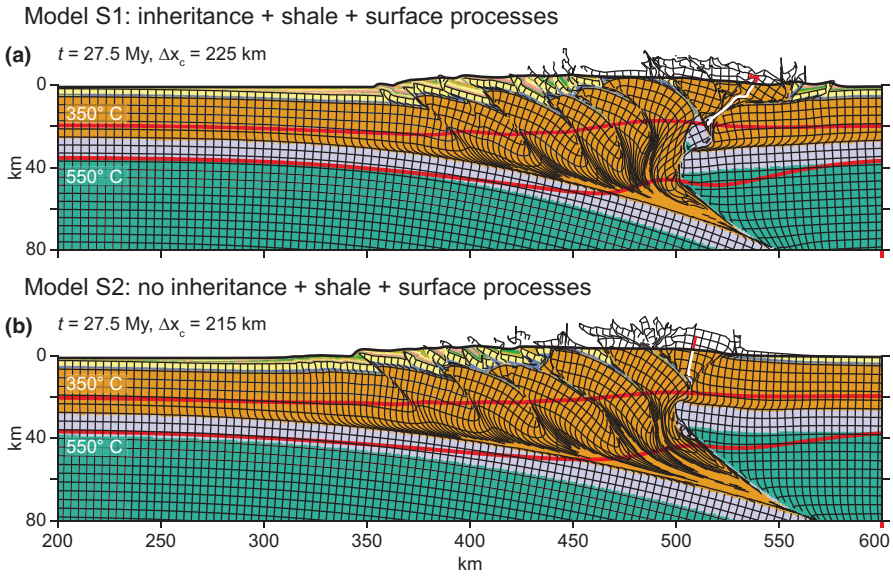

FIGURE 3 Compilation of supplementary models after 27.5 My. (a) Model S1, with a frictional shale décollement ($\phi_{eff} = 2°$), does not feature gravitational collapse of the cover. (b) Model S2, with a frictional shale décollement and without extensional inheritance, is highly asymmetric and its retro-wedge is limited to a single low-offset shear zone

similar to Model 1. Model S2 has no rift inheritance and features the same frictional décollement as Model S1 (Figure 3b). The first shear zone that cuts through the crust and lithospheric mantle is inclined, immediately creating the subduction asymmetry resulting in a highly asymmetric orogen with a wide pro-wedge and negligible retro-wedge shortening. The pro-wedge deformation style is the same as in S1.

3.2 | Shortening distribution

Quantitative analysis of the shortening distribution between the pro- and retro-wedges reveals that both models with rift inheritance show a very similar shortening distribution. Initial inversion during Phase 1 is roughly symmetric (Figure 4a). After Phase 1 the retro-wedge is briefly abandoned and then reactivated in Phase 2. During asymmetric orogenic growth in Phase 2, the shortening rate of the retro-wedge is only ~18%-20% of the overall convergence rate, with deformation focussed into the pro-wedge. Overall, rift inheritance models accommodate more shortening in the retro-wedge than the model without extensional inheritance, stabilising at around 18%-20% of total convergence after ~100 km (Figure 4c). In Model S2 (no inheritance) shortening is quickly concentrated almost exclusively into the pro-wedge and retro-wedge shortening stabilises to around 6% of total convergence after only 50 km.

4 | DISCUSSION

Model 1 shows that a highly mobile cover in combination with surface processes is sufficient to promote formation of a crustal antiformal stack. A weak salt décollement allows efficient decoupling

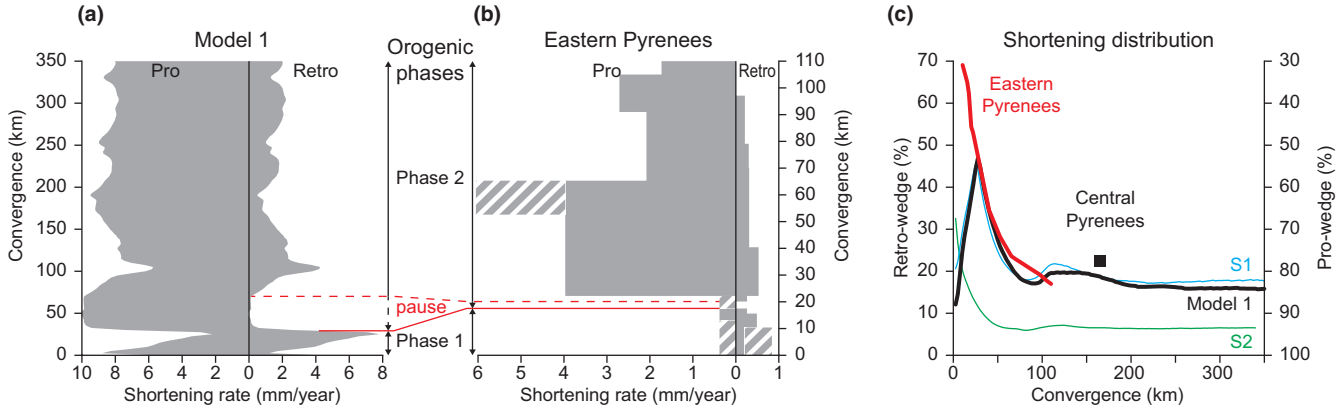

FIGURE 4 (a) Pro- and retro-wedge shortening rate of Model 1, plotted against total convergence. (b) Pro-and retro-wedge shortening rate of the Eastern Pyrenees, plotted against total convergence (note difference in scale). (c) Shortening distribution between the pro- and retro-wedges, plotted against total convergence. Central Pyrenean data (black box) from Beaumont et al. (2000). East Pyrenean data from Grool et al. (2018)

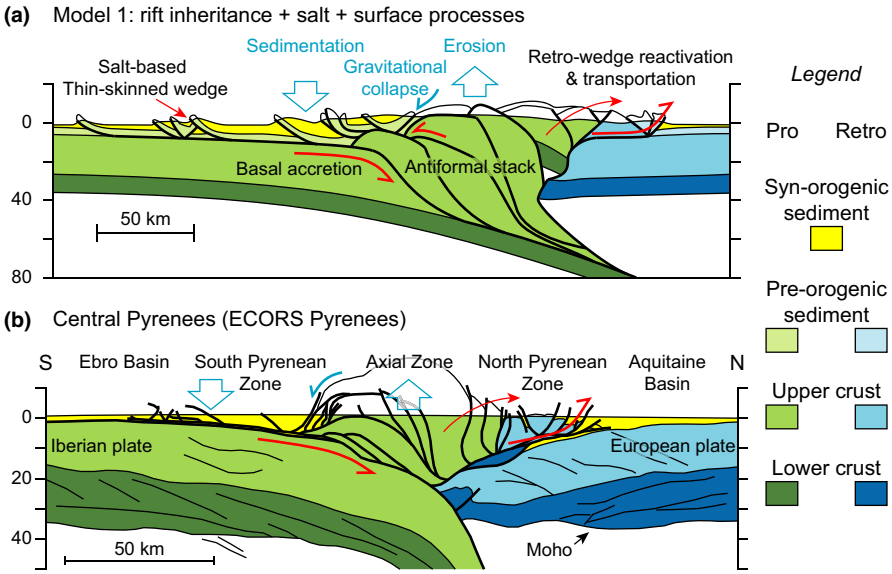

FIGURE 5 (a) Cartoon of Model 1 after 225 km of convergence showing factors (in blue) driving basal accretion and growth of an antiformal stack. The retro-wedge is reactivated and transported by over-steepened trailing edge pro-wedge thrust sheets migrating onto the upper plate as the antiformal stack grows. (b) Cartoon of Central Pyrenees showing the same mechanism of shallow structure forcing underthrusting, growth of an antiformal stack, and reactivation of the retro-wedge. This section does not distinguish between pre- and syn-orogenic sediments. Modified after Muñoz (1992) and Beaumont et al. (2000)

of the cover. Together with the mid-crustal décollement, this forms a system of stacked, interacting décollements or nested critical wedges. The salt décollement cannot support the high surface slope necessary for the critical taper associated with the mid-crustal décollement, leading to gravitational collapse of the cover. Combined with surface processes that further reduce the surface slope (e.g., Storti & McClay, 1995; Willett, 1999), the thick-skinned pro-wedge taper is subcritical, promoting thick-skinned underthrusting in the core of the orogenic wedge (Rushlow et al., 2013; Sinclair et al., 2005). This, in turn, again generates gravitational collapse of cover on the uplifting crustal antiformal stack. This positive feedback loop promotes an antiformal stack flanked by a wide low taper thin-skinned fold-and-thrust belt in the pro-wedge (Figure 5a). This structure emerges naturally in our model, not relying on prescribed weak zones and S-point (Beaumont et al., 2000) or a hinterland that is even thicker than the antiformal stack itself (Malavieille, 2010) to force formation of an antiformal stack. With a more competent frictional décollement, the fold-and-thrust belt cannot gravitationally collapse, thus avoiding the feedback loop that generates a crustal-scale antiformal stack (Models S1, S2). Thus, only a salt décollement combined with surface processes can promote formation of a crustal-scale antiformal stack. With less effective crustal strain weakening, this effect may not be sufficient to generate an antiformal stack.

Model 1 also shows that a two-phase shortening distribution is primarily controlled by rift inheritance. In Model 1 the early symmetric inversion (Phase 1) is caused by the pre-existing rift symmetry. In Phase 2 strain weakening and geometrical incompatibility of the two shear zones promotes asymmetric shear localisation in the lithospheric mantle upon collision of the intact lower crust and lithospheric mantle. Without rift inheritance, asymmetric shortening is established from the moment the first lithospheric shear zone is formed, effectively skipping Phase 1 entirely (Model S2).

In all our models, the onset of asymmetric shortening distribution in the upper crust (Phase 2) coincides perfectly with the onset of asymmetric subduction of the lithospheric mantle. All models with rift inheritance accommodate ~80% of shortening in the pro-wedge, regardless of thin-skinned décollement rheology. This suggests that it is the subduction asymmetry in the lithospheric mantle that controls shortening distribution in the upper crust. Thus, one could use the onset of asymmetric shortening to date the onset of lower lithosphere subduction.

5 | PYRENEAN DOUBLY-VERGENT OROGEN

Here, we compare the geometry and evolution of Model 1 to the Pyrenean orogen (Figure 5b). The Pyrenees are often used as a type example of a mountain belt that resulted from inversion of a salt-rich, narrow, mantle-exhuming rift (e.g., Muñoz, 1992; Jammes, Manatschal, Lavier, & Masini, 2009).

The crustal antiformal stack in the Pyrenean Axial Zone exhibits nearly complete overlap between thrust sheets (Figure 5b) (Muñoz, 1992). Model 1 reproduces this antiformal stack geometry (Figure 5a). The same factors that promote an antiformal stack in Model 1 are found in the Pyrenees: Erosion efficiently removes mass from the central orogen (e.g., Rushlow et al., 2013); Sedimentation adds mass to the forelands (e.g., Sinclair et al., 2005); Thrusting of the cover above a salt décollement allows mass to migrate outward, particularly in the pro-wedge, to form a wide fold-and-thrust belt (e.g., Cámara & Flinch, 2017; Vergés et al., 1998).

The evolution of the shortening distribution in the Eastern Pyrenees, based on a thorough field study and balanced cross-sections (Grool et al., 2018), fits remarkably well with that of our models that include rift inheritance (Models 1 and S1), both qualitatively and quantitatively (Figure 4, note different scale of panels a and b). Phase 1 shortening in the Eastern Pyrenees is characterised by roughly symmetric rift inversion. Phase 2 is initiated simultaneously with the onset of asymmetric subduction of the lithospheric mantle, resulting in temporary abandonment of the

retro-wedge. Over-steepening of the growing pro-wedge trailing edge allows the upper thrust sheets to migrate onto the upper plate, reactivating the retro-wedge albeit modestly. Pyrenean shortening is distributed roughly 80% and 20% between the pro- and retro-wedges, respectively, as in Models 1 and S1.

The depth of the mid-crustal décollement in the reconstruction of Muñoz (1992) is significantly shallower than in our models. However, we did not set out to fully reproduce all details of the Pyrenees, and the depth of this décollement remains poorly constrained. Changing the depth of this décollement would probably not significantly change our main findings.

The combined effects of a highly mobile cover, orogen erosion and foreland sedimentation may also explain antiformal stack-like structures in the Central Alps (Schmid et al., 2017) and in the frontal zone of the Himalayas (Mercier, Braun, & Beek, 2017).

6 | CONCLUSIONS

Our numerical modelling results show that the presence of a weak viscous (salt) décollement can strongly control crustal deformation in a convergent orogen. The development of a crustal-scale antiformal stack is promoted by the combined effects of gravitational collapse of the cover above the salt décollement off the uplifting orogenic core, efficient erosion of the orogenic core and deposition of sediments in the foreland. Rift inheritance results in a two-phase orogenic evolution, with Phase 1 symmetric rift inversion and Phase 2 asymmetric main collision, triggered by asymmetric subduction of the lithospheric mantle. The onset of asymmetric shortening can be used to date the onset of subduction. Comparison to the Pyrenees shows that these controlling factors and resulting geometries are found in nature.

ACKNOWLEDGEMENTS

This research was funded by the French ANR project PYRAMID. Computing hours are part of SIGMA2 high performance computing allocation project NN4704K: 3D forward modelling of lithosphere extension and inversion. Ritske Huismans thanks and is indebted to Josep Anton Muñoz for sharing his insights into Pyrenean geology and for highly fruitful discussions. This is CRPG publication nr. 2722

ORCID

Arjan R. Grool https://orcid.org/0000-0002-6853-0804
Ritske S. Huismans https://orcid.org/0000-0003-0548-6591
Mary Ford https://orcid.org/0000-0002-8343-188X

REFERENCES

Beaumont, C., Muñoz, J. A., Hamilton, J., & Fullsack, P. (2000). Factors controlling the Alpine evolution of the central Pyrenees inferred from a comparison of observations and geodynamical models. *Journal of Geophysical Research*, *105*, 8121–8145. https://doi.org/10.1029/1999JB900390

Burg, J. P., & Gerya, T. V. (2005). The role of viscous heating in Barrovian metamorphism of collisional orogens: thermomechanical models and application to the Lepontine Dome in the Central Alps. *Journal of Metamorphic Geology*, *23*, 75–95. https://doi.org/10.1111/j.1525-1314.2005.00563.x

Cámara, P., & Flinch, J. F. (2017). The Southern Pyrenees: A salt-based fold-and-thrust belt. In J. I., Soto, J. F. Flinch & G. Tari (Eds.), *Permo-Triassic Salt Provinces of Europe, North Africa and the Atlantic Margins* (pp. 395–415). Amsterdam, the Netherlands: Elsevier. https://doi.org/10.1016/B978-0-12-809417-4.00019-7

Davis, D. M., & Engelder, T. (1985). The role of salt in fold-and-thrust belts. *Tectonophysics*, *119*, 67–88. https://doi.org/10.1016/0040-1951(85)90033-2

Erdős, Z., Huismans, R. S., & van der Beek, P. (2015). First-order control of syntectonic sedimentation on crustal-scale structure of mountain belts. *Journal of Geophysical Research: Solid Earth*, *120*, 1–16. https://doi.org/10.1002/2014JB011785

Erdős, Z., Huismans, R. S., van der Beek, P., & Thieulot, C. (2014). Extensional inheritance and surface processes as controlling factors of mountain belt structure. *Journal of Geophysical Research: Solid Earth*, *119*, 9042–9061. https://doi.org/10.1002/2014JB011408

Faccenda, M., Gerya, T. V., & Chakraborty, S. (2008). Styles of post-subduction collisional orogeny: Influence of convergence velocity, crustal rheology and radiogenic heat production. *Lithos*, *103*, 257–287. https://doi.org/10.1016/j.lithos.2007.09.009

Ford, M. (2004). Depositional wedge tops: interaction between low basal friction external orogenic wedges and flexural foreland basins. *Basin Research*, *16*, 361–375. https://doi.org/10.1111/j.1365-2117.2004.00236.x

Grool, A. R., Ford, M., Vergés, J., Huismans, R. S., Christophoul, F., & Dielforder, A. (2018). Insights into the crustal-scale dynamics of a doubly vergent orogen from a quantitative analysis of its forelands: A case study of the Eastern Pyrenees. *Tectonics*, *37*, 450–476. https://doi.org/10.1002/2017TC004731

Jammes, S., & Huismans, R. S. (2012). Structural styles of mountain building: Controls of lithospheric rheologic stratification and extensional inheritance. *Journal of Geophysical Research: Solid Earth*, *117*, B10403. https://doi.org/10.1029/2012JB009376

Jammes, S., Manatschal, G., Lavier, L. L., & Masini, E. (2009). Tectonosedimentary evolution related to extreme crustal thinning ahead of a propagating ocean: Example of the western Pyrenees. *Tectonics*, *28*, TC4012. https://doi.org/10.1029/2008TC002406

Malavieille, J. (2010). Impact of erosion, sedimentation, and structural heritage on the structure and kinematics of orogenic wedges: Analog models and case studies. *GSA Today*, *20*, 4–10. https://doi.org/10.1130/GSATG48A.1

Mercier, J., Braun, J., & van der Beek, P. (2017). Do along-strike tectonic variations in the Nepal Himalaya reflect different stages in the accretion cycle? Insights from numerical modelling. *Earth and Planetary Science Letters*, *472*, 299–308. https://doi.org/10.1016/j.epsl.2017.04.041

Mitra, G., & Boyer, S. E. (1986). Energy balance and deformation mechanisms of duplexes. *Journal of Structural Geology*, *8*, 291–304. https://doi.org/10.1016/0191-8141(86)90050-7

Muñoz, J. A. (1992). Evolution of a continental collision belt: ECORS-Pyrenees crustal balanced cross-section. In K. R. McClay (Ed.), *Thrust tectonics* (pp. 235–246). Dordrecht, the Netherlands: Springer, Netherlands. https://doi.org/10.1007/978-94-011-3066-0_21

Nilfouroushan, F., Pysklywec, R., Cruden, A. R., & Koyi, H. A. (2013). Thermal-mechanical modeling of salt-based mountain belts with pre-existing basement faults: Application to the Zagros fold and thrust belt, southwest Iran. *Tectonics*, *32*, 1212–1226. https://doi.org/10.1002/tect.20075

Rushlow, C. R., Barnes, J. B., Ehlers, T. A., & Vergés, J. (2013). Exhumation of the southern Pyrenean fold-thrust belt (Spain) from orogenic growth to decay. *Tectonics*, *32*, 843–860. https://doi.org/10.1002/tect.20030

Schmid, S. M., Kissling, E., Diehl, T., van Hinsbergen, D. J. J., & Molli, G. (2017). Ivrea mantle wedge, arc of the Western Alps, and kinematic evolution of the Alps-Apennines orogenic system. *Swiss Journal of Geosciences*, *110*, 581–612. https://doi.org/10.1007/s00015-016-0237-0

Sinclair, H. D., Gibson, M., Naylor, M., & Morris, R. G. (2005). Asymmetric growth of the Pyrenees revealed through measurement and modeling of orogenic fluxes. *American Journal of Science*, *305*, 369–406. https://doi.org/10.2475/ajs.305.5.369

Storti, F., & McClay, K. (1995). Influence of syntectonic sedimentation on thrust wedges in analogue models. *Geology*, *23*, 999-1002. https://doi.org/10.1130/0091-7613(1995)023<0999:IOSSOT>2.3.CO;2

Thieulot, C. (2011). FANTOM: Two- and three-dimensional numerical modelling of creeping flows for the solution of geological problems. *Physics of the Earth and Planetary Interiors*, *188*, 47–68. https://doi.org/10.1016/j.pepi.2011.06.011

Vergés, J., Marzo, M., Santaeulària, T., Serra-Kiel, J., Burbank, D. W., Muñoz, J. A., & Giménez-Montsant, J. (1998). Quantified vertical motions and tectonic evolution of the SE Pyrenean foreland basin. In A. Mascle, C. Puigdefàbregas, H. P. Lutherbacher, & M. Fernàndez (Eds.), *Cenozoic foreland Basins of Western Europe 134*, 107–134. London, UK. Geological Society of London: Geological Society Special Publications. https://doi.org/10.1144/GSL.SP.1998.134.01.06

Warren, C. J., Beaumont, C., & Jamieson, R. A. (2008). Deep subduction and rapid exhumation: Role of crustal strength and strain weakening in continental subduction and ultrahigh-pressure rock exhumation. *Tectonics*, *27*. https://doi.org/10.1029/2008TC002292

Willett, S. D. (1999). Orogeny and orography: The effects of erosion on the structure of mountain belts. *Journal of Geophysical Research*, *104*, 28957–28981. https://doi.org/10.1029/1999JB900248

SUPPORTING INFORMATION

Additional supporting information may be found online in the Supporting Information section at the end of the article.

Data S1. Supplementary methods and model descriptions.

How to cite this article: Grool AR, Huismans RS, Ford M. Salt décollement and rift inheritance controls on crustal deformation in orogens. *Terra Nova*. 2019;31:562–568. https://doi.org/10.1111/ter.12428